

OPTIMUM LAY-UP DESIGN ANALYSIS OF
BASALT FIBER REINFORCED COMPOSITE USING
FINITE ELEMENT ANALYSIS (FEA)

MUHAMAD HANIF MUQSIT BIN AZHAR

MECHANICAL ENGINEERING
UNIVERSITI TEKNOLOGI PETRONAS
MAY 2014

**Optimum Lay-Up Design Analysis of Basalt Fiber Reinforced Composite Using
Finite Element Analysis (FEA)**

by

Muhamad Hanif Muqsit bin Azhar
13185

Dissertation submitted in partial fulfillment of
the requirements for the
Bachelor of Engineering (Hons)
(Mechanical Engineering)

MAY 2014

Universiti Teknologi PETRONAS
Bandar Seri Iskandar
31750 Tronoh
Perak Darul Ridzuan

CERTIFICATION OF APPROVAL

**Optimum Lay-Up Design Analysis of Basalt Fiber Reinforced Composite Using
Finite Element Analysis (FEA)**

by

Muhamad Hanif Muqsit bin Azhar

13185

Dissertation submitted in partial fulfillment of
the requirements for the
Bachelor of Engineering (Hons)
(Mechanical Engineering)

Approved by,

(Dr Saravanan Karuppanan)

UNIVERSITI TEKNOLOGI PETRONAS
TRONOH, PERAK
MAY 2014

CERTIFICATION OF ORIGINALITY

This is to certify that I am responsible for the work submitted in this project, that the original work is my own except as specified in the references and acknowledgements, and that the original work contained herein have not been undertaken or done by unspecified sources or persons.

(MUHAMAD HANIF MUQSIT BIN AZHAR)

ABSTRACT

In this study, the focus was on the optimum design of laminate stacking sequences (LSS) of basalt fiber reinforced composite (BFRP). Composite is a combination of two or more materials, which are commonly known as reinforcement and matrix. As for this project, basalt was selected as the reinforcement since this material still need a thorough study before it can be used for application, while epoxy was used as the matrix. There are many factors that could affect the properties of a composite such as fiber matrix bond, the type and volume of fiber, the distribution and orientation of fiber within the matrix, the ability to obtain isotropic and orthotropic behavior if required, ease of handling of the reinforcement and a suitable method for manufacture. Because of these factors, the mechanical properties of a composite might be different from each other. For that reasons, the analysis for BFRP has been conducted by Finite Element Analysis (FEA) software, ANSYS Composite Pre-Post (ACP). Firstly, the simulation was validated with previous experiment conducted in the selected literature. A nonlinear simulation for three-point flexural test was done for the validation purpose and the results obtained from the simulation were compared with the experimental results from literature. From the result, it was shown that the plotted line of load-displacement graph for ANSYS result was acceptable. Then, the simulation was extended to the designing of different layup sequences of basalt fiber reinforced composite (BFRP) which was aimed for maximum strength and stiffness. Several combinations of different orientation angles were introduced on the layers, and the results obtained showed that the increase in orientation angle θ leads to the decrease in composite stiffness. Stress-strain curve of the results were plotted for further analysis.

ACKNOWLEDGEMENT

First and foremost, I would like to express the greatest gratitude to Allah S.W.T for lending me a good health, strength, opportunity and blessing throughout the completion of my Final Year Project.

I would like to capture this moment to convey my special appreciation to the individuals who gave the supports and cooperation, especially to my supervisor Dr. Saravanan Karuppanan and Mr. Ali Nawaz for their guidance, help and constant encouragement throughout the entire project. Without their advices and opinions surely it will be hard for me to be able to complete this project.

A sincere appreciation and millions of thanks to my beloved parent and family members, who never stop believing in me and always cheer me up, lend me their strength and pray for me during my study in Universiti Teknologi PETRONAS. I do acknowledge all the supports given and I wanted to deliver my success as a present for them.

Last but not least, my special thanks to all my friends and colleagues for their help in many ways. Thank you very much.

TABLE OF CONTENTS

ABSTRACT	iv
ACKNOWLEDGEMENT	v
LIST OF FIGURES	vii
LIST OF TABLES	ix
CHAPTER 1:	INTRODUCTION	1
	1.1 Background	1
	1.2 Problem Statement	2
	1.3 Objectives	3
	1.4 Scope of Study	3
CHAPTER 2:	LITERATURE REVIEW	4
	2.1 Comparison of Materials Properties	4
	2.2 Effect of LSS on Composite Properties	6
CHAPTER 3:	METHODOLOGY	13
	3.1 Project Flow	13
	3.2 Project Methodology	14
	3.3 Designing Layup Stacking Sequence	17
	3.4 Progress Summary and Milestone	22
CHAPTER 4:	RESULT AND DISCUSSION.	25
	4.1 Result Validation with Carbon Fiber	25
	4.2 Benchmarking of Results	26
	4.3 Results for LSS of BFRP	28
CHAPTER 5:	CONCLUSION AND RECOMMENDATIONS	31
REFERENCES	32
APPENDICES	34

LIST OF FIGURES

Figure 1.1:	Volcanic basalt rock	2
Figure 2.1:	Heat deflection temperature and Vicat softening temperatures of BF/PBS composites with various basalt fiber content	6
Figure 2.2:	Schematic illustrations of laminates with various layup sequences	7
Figure 2.3:	Comparison of tensile, flexural and compressive Young's modulus between basalt and E-glass fiber composites	8
Figure 2.4:	Comparison of tensile, flexural and compressive ultimate strength between basalt and E-glass fiber composites	8
Figure 2.5:	The effect of different stacking sequence with a fixed ply number	9
Figure 2.6:	(a) Maximum tensile stress for different LSS orientation and ply number	10
	(b) Maximum tensile stress for different ply number with same LSS orientation of [0/30/60]	10
Figure 2.7:	Variation of failure loads with fiber orientation angle	11
Figure 2.8:	Variation of tensile modulus with fiber orientation angle	11
Figure 2.9:	Different stacking sequences of carbon (C) and basalt (B) fiber plies	12
Figure 2.10:	Average flexural strength and modulus of CFRP, BFRP and interply hybrid composites with different stacking sequences	12
Figure 3.1:	Flow of the project	13
Figure 3.2:	Dimension of the carbon/epoxy composite	15
Figure 3.3:	Static structural stand-alone analysis	16
Figure 3.4:	ANSYS engineering data for defining materials properties	16
Figure 3.5:	Importing the composite geometry	17
Figure 3.6:	Meshing of the composite	17
Figure 3.7:	Simple support applied (blue color)	18
Figure 3.8:	Steps control setting	18
Figure 3.9:	Tabular data for force applied	18
Figure 3.10:	Force applied on the composite (red color)	19
Figure 3.11:	Inserting total deformation under solution branch	19
Figure 3.12:	Example of the simulation result on the composite	20

Figure 3.13:	Static structural stand-alone analysis with ANSYS Composite Pre-Processing (ACP)	21
Figure 3.14:	ANSYS composite pre-post (ACP) setting for layer thickness	22
Figure 3.15:	ANSYS composite pre-post (ACP) setting for fiber orientation	22
Figure 3.16:	Layers of the composite	23
Figure 3.17:	0° fiber orientation	23
Figure 3.18:	45° fiber orientation	23
Figure 3.19:	60° fiber orientation	24
Figure 3.20:	90° fiber orientation	24
Figure 4.1:	Load versus displacement graph for result validation	27
Figure 4.2:	Load versus displacement comparison for BFRP, GFRP and CFRP	29
Figure 4.3:	Stress-strain curve for BFRP, GFRP and CFRP	30
Figure 4.4:	Stress-strain curve for alternate and alternate symmetrical fiber orientation	31
Figure 4.5:	Stress-strain curve for random symmetrical fiber orientation	31

LIST OF TABLES

Table 2.1:	Basalt fiber properties, comparisons with glass and carbon fibers Properties	4
Table 2.2:	Thermal properties comparisons for basalt fiber and glass fiber	5
Table 2.3:	Laminates stacking sequences for basalt and glass	7
Table 3.1:	Properties for Carbon/Epoxy, Basalt/Epoxy and Glass/Epoxy composite	14
Table 3.2:	Dimensions for the composite	15
Table 3.3:	Layup stacking sequences for each sample	21
Table 3.4:	Gantt chart, milestones and project activities for FYP1	25
Table 3.5:	Gantt chart, milestones and project activities for FYP2	26
Table 4.1:	Results comparison	28

CHAPTER 1

INTRODUCTION

1.1 Background of Study

Composite materials are generally defined as a combination of two or more constituent materials which have different properties. By doing so, a new material is fabricated with new and additional mechanical properties. Usually, the aims for producing composites are to obtain a strong, stiff and lightweight material [1]. Two main components of a composite material are matrix and reinforcement. When the composite is subjected to forces, the matrix would transfer the stresses to disperse phase, and also protect the reinforcement. On the other hand, the primary role of reinforcement in composite material is to enhance the mechanical properties of the material.

Many types of reinforcement are being used in producing a composite, and the most famously used reinforcements are carbon and glass. In composite manufacturing process, these reinforcements are in fiber form. Carbon fibers and glass fibers are widely adopted in the composite industry due to their superior properties such as good strength-to-weight ratio, high modulus of elasticity and density [2]. Because of these reasons, composite is enchanting for various application such as automotive industry, civil structures, aircraft, marine and public work industries.

Recently, the attentions in composite industry are to produce a composite with a lower cost and also biodegradable. Carbon fiber is known for its expensive price compared to the other fibers such as glass fibers and kenaf fibers. However, the mechanical properties of these two fibers are not as good as carbon fibers eventhough their price is much affordable. These issues can be solved by using a new mineral fiber which is basalt [3]. Basalt fiber is a newcomer in composites industry and a possible candidate that could be commercialized due to its good mechanical properties and potentially low cost [4]. Basalt as shown in Figure 1.1 is a type of volcanic rock that emerged from the earth surface during volcanic eruption and it was formed from a rapid cooling process of the basaltic lava. Besides, a large area of ocean floor is also covered with this abundant rock [5].



Figure 1.1: Volcanic basalt rock [6]

Since basalt fiber is still young in the composite field, a lot of studies and researches have to be done to determine the performances of this fiber. The most important parameters that could affect the mechanical properties of a composite are fiber matrix bond, the type and volume of fiber, the distribution and orientation of fiber within the matrix, the ability to obtain isotropic and orthotropic behavior if required, ease of handling of the reinforcement and a suitable method for manufacture [7]. As for this project, the intention would be to find the optimum layup design and orientation of basalt fiber reinforced composite (BFRP) by comparing the mechanical properties values.

1.2 Problem Statement

Appropriate and acceptable properties of fiber reinforced composite (FRP) must be selected to suit with the applications. Mostly FRP products were produced in the forms of composite that have different number of layers and orientations. Because of that, the mechanical properties of the FRP would be different and correct selection has to be made. Basalt fiber has to be further analyzed as it is a new comer in the FRP industry.

Therefore, it appears to be very important to design and model the layup stacking sequences (LSS) and orientations of BFRP by using Finite Element Analysis (FEA) to analyze the outcome thoroughly.

1.3 Objective

Various LSS and orientation would result in different outcome from the FEA simulation. Significantly, these following objectives would be helpful to understand the behavior and properties of BFRP.

1. Design and model of different kinds of basalt fiber layup.
2. Analyze the stress distribution of the layup schemes.
3. Determine the optimum layup design which aim for maximum strength and stiffness.

1.4 Scope of Study

The project would be focusing on Finite Element Analysis (FEA) of basalt fiber reinforced composite (BFRP) by using ANSYS software as the simulation tool. The FEA will be done by simulating the flexural test of BFRP according to ASTM D790 with different stacking sequences. The scope of the project is achievable within the time frame given for the final year project, which is for two semesters. It is not a time-consuming project; therefore time frame is not a factor for the project.

CHAPTER 2

LITERATURE REVIEW

2.1 Comparison of Materials Properties

Mostly fiber reinforced composites are produced with the aim to obtain better mechanical properties. It was claimed that basalt fiber has the potential to be an alternative material instead of carbon that is more costly and also glass fiber, which has lower mechanical properties [8]. From Table 2.1, it was noticed that the tensile strength for basalt fiber is way better than carbon fibers, but slightly higher than S-glass fiber. In a simple word, basalt fiber would have an excellent resistance from breaking when subjected to tensile load. Eventhough glass fibers are definitely cheaper than basalt fibers in terms of price per kilogram in 2007, but they have low properties compared to basalt fibers properties. Comparing the price for basalt and carbon, it can be seen clearly that carbon is USD27.5 more expensive than basalt. For that reason, basalt would be more affordable with higher mechanical properties than carbon. According to Burger in his report for Reuters [9], the price for carbon fiber in 2014 is 140 USD/ kg, which is way too expensive compared to basalt fiber that cost only around 1.5-5.4 USD/kg [10].

Table 2.1: Basalt fiber properties, comparisons with glass and carbon fibers properties [5,11]

Properties	Material				
	Basalt	E-glass	S-glass	Carbon (high strength)	Carbon (high modulus)
Tensile Strength (MPa)	4840	3450	4580	3500	2500-4000
Elastic Modulus (MPa)	89,000	72,400	85,500	240,000	350,000- 650,000
Elongation at break (%)	3.1	4.7	5.6	1.25	0.5
Density (g/cm^3)	2.8	2.6	2.5	1.75	1.95
Price (year 2007) (USD/kg)	2.5	1.1	1.5	30	-

Table 2.2: Thermal properties comparisons for basalt fiber and glass fiber [5,11]

Properties	Basalt	Glass
Maximum application temperature (°C)	982	650
Sustained operating temperature (°C)	820	480
Minimum operating temperature (°C)	-260	-60
Thermal conductivity (W/mK)	0.031-0.038	0.034-0.04
Thermal expansion coefficient (ppm/°C)	8	5.4

Moving on with the thermal aspect as shown in Table 2.2, all the thermal properties are in favor of basalt fiber. Basalt fiber provides good heat resistance with higher maximum application temperature and lower thermal conductivity than glass fibers. Moreover, basalt fiber also exhibits good performance at high temperature which makes it more preferable nowadays.

Figure 2.1 shows heat deflection temperature and Vicat softening temperature of basalt fiber reinforced poly (butylene succinate) composite (BF/PBS), and it is clearly illustrated that the heat deflection temperature for (BF/PBS) is increased by 40% from 82°C to 114°C while Vicat softening temperature also increased from 96°C to 109°C with increasing content of basalt fiber [11]. With this result, it was noticed that basalt fiber is a good material as an alternative to the other high temperature resistance fiber such as carbon, where the main applications of this property are in heat shields and fire protection in thermal insulating barrier [5].

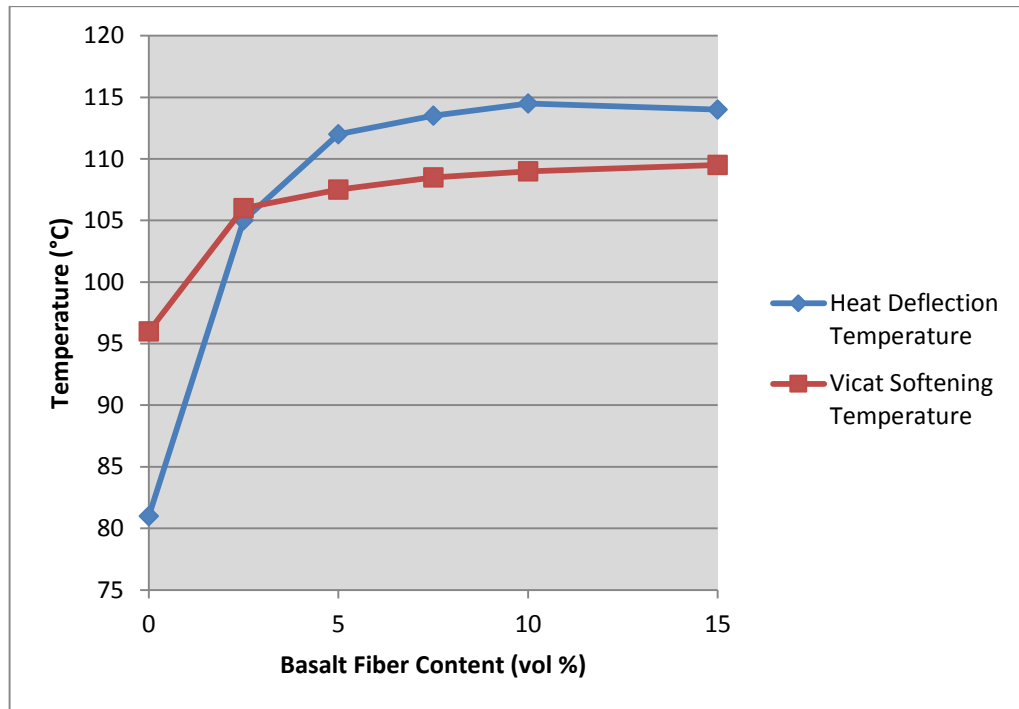


Figure 2.1: Heat deflection temperature and Vicat softening temperatures of BF/PBS composites with various basalt fiber content [11]

On the other hand, the natural fiber of basalt is also better in terms of chemical properties as compared to other glass fibers. Basalt fiber does not release any chemical elements when heated since no additives or solvents are needed during the production process [5]. In addition, basalt is also more resistant to acid and alkali, can withstand less degradation by water and alkalis [5]. Because of that, it could be said that the production process of basalt fiber is completely environmental friendly, and it could be recycled.

2.2 Effect of Laminate Stacking Sequences (LSS) on Composite Properties

Before being widely used in the applications, BFRP might be produced or manufactured in laminates form. Usually, laminates of the fibers are made of several types of layup sequences and fiber orientation in order to enhance the properties of the laminate composites. The reason for this purpose is to allow the laminate to behave like anisotropic material even though some of the layers are isotropic [12].

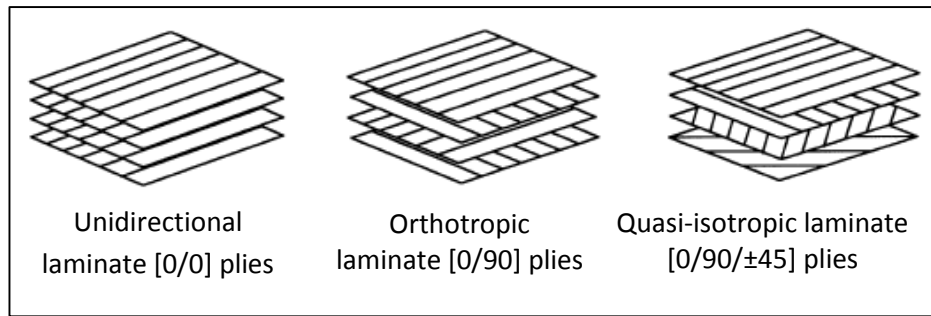


Figure 2.2: Schematic illustrations of laminates with various layup sequences [12]

There are three types of common laminates that are made up of different layer orientations as shown in Figure 2.2. These three types of laminates would behave differently from each other if subjected with the same load. Because of that, proper selection must be made since the properties of these laminates are not the same due to the layer sequence and orientation. More than that, the number of layup layer can also be added symmetrically or unsymmetrically. Therefore, it is important to predict and observe the behavior of BFRP with the aim to find the optimum layup design with maximum strength.

Table 2.3: Laminates stacking sequences for basalt and glass [3]

Test	Standard Test Method	Reinforcement	Stacking Sequence	Thickness (mm)
Tensile	ASTM D3039	Basalt	$[0/9]_{16}$	2.5
		Glass	$[0/90]_8$	2.5
Compression	ASTM D695	Basalt	$[0/90]_{25}$	12.7
		Glass	$[0/90]_{20}$	12.7
Flexural	ASTM D790	Basalt	$[0/90]_{16}$	2.6
		Glass	$[0/90]_{10}$	2.6

Some previous studies prove that different LSS will affect the properties of the composites. Table 2.3 indicates the stacking sequences of the composites used for comparison of Young's modulus, obtained for BFRP and GFRP from three different experiments which are tensile test, flexural test and compression test. It was shown in Figure 2.3 that the Young's modulus values for BFRP are significantly higher, 35%~45% higher than GFRP [3]. It was observed that the difference in LSS played an important role in the results obtained.

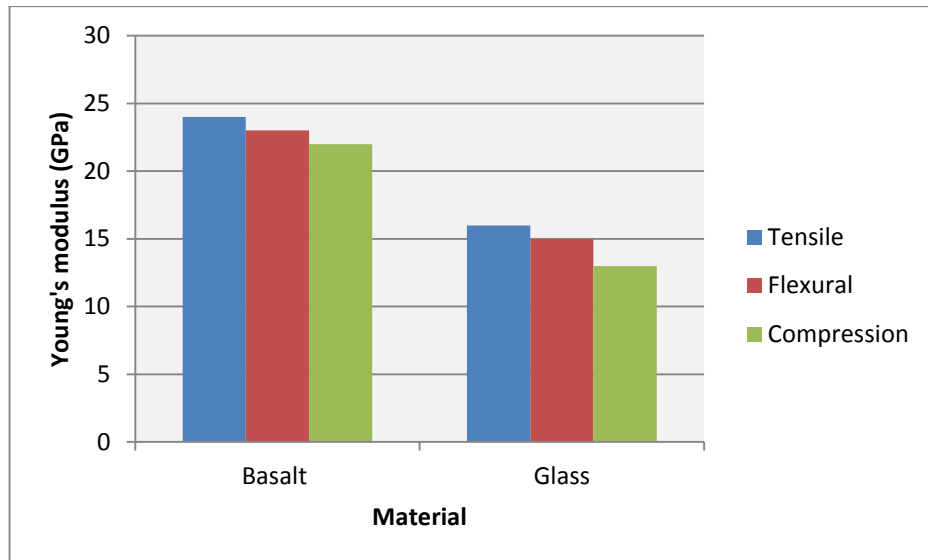


Figure 2.3: Comparison of tensile, flexural and compressive Young's modulus between basalt and E-glass fiber composites [3]

Meanwhile, the results for ultimate strength for both composites show some contradiction. It can be seen from Figure 2.4 that the glass composite showed better result for ultimate strength when subjected to tensile test. However, flexural and compression test still showed that basalt has better ultimate strength than glass. As quoted by Lopresto *et al.* [3], "It is possible to observe that basalt fiber reinforced plastics showed similar tensile and bending strength, meaning that the major bending failure happened in tensile way. The same did not happen for glass fiber specimen that showed different and very low flexural and compressive ultimate strength compared to the basalt ones."

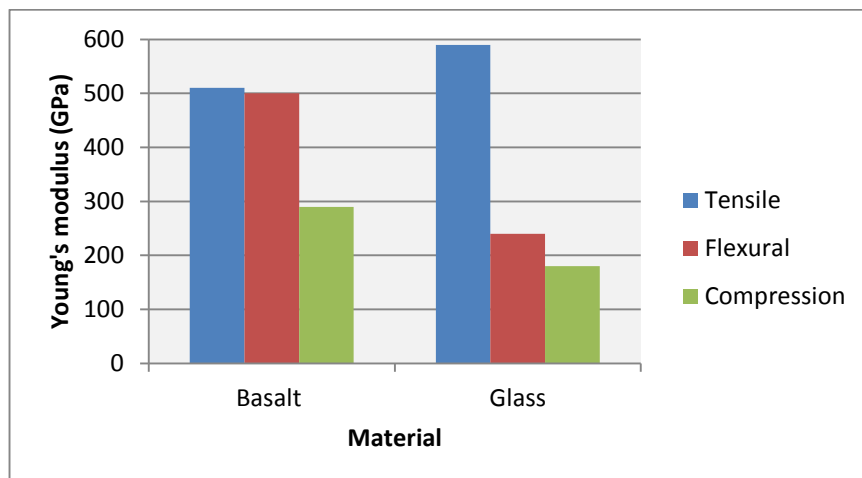


Figure 2.4: Comparison of tensile, flexural and compressive ultimate strength between basalt and E-glass fiber composites [3]

This indicates that the bending failure mechanism for both fibers is different. All the results for this experiment was obtained by using the same stacking sequences angles which were 0° and 90° while the number of plies were designed to match the same thickness for both composite. On the other hand, other study [13] had been conducted to investigate the properties of composite when subjected to different LSS angles while maintaining the layup numbers. Figure 2.5 shows the effective elastic modulus in X-direction obtained for Nicalon/SiC composite according to the stacking sequences as in Table 2.4. The results show that various elastic modulus were obtained for different LSS with the same ply number.

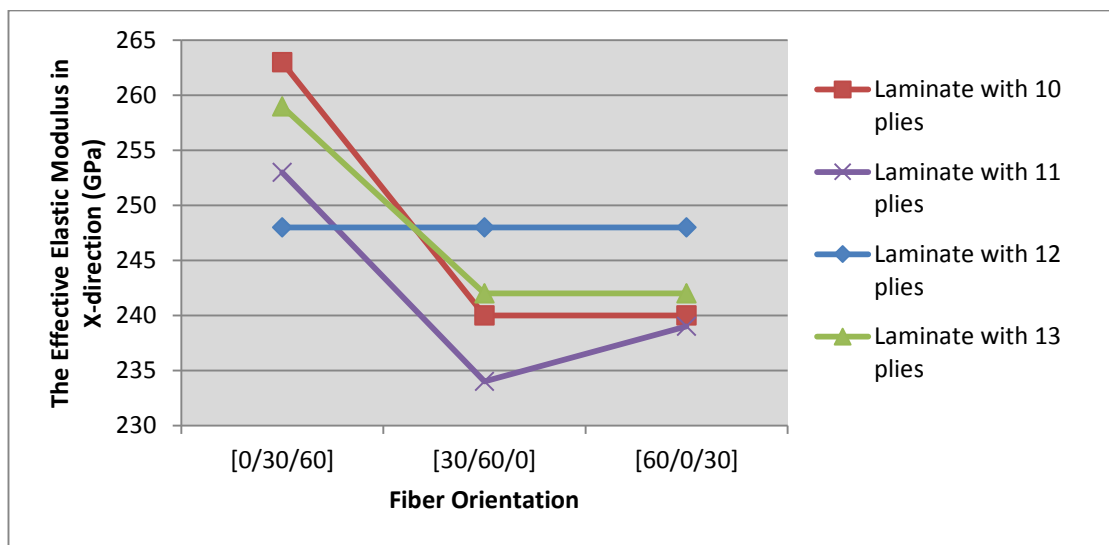
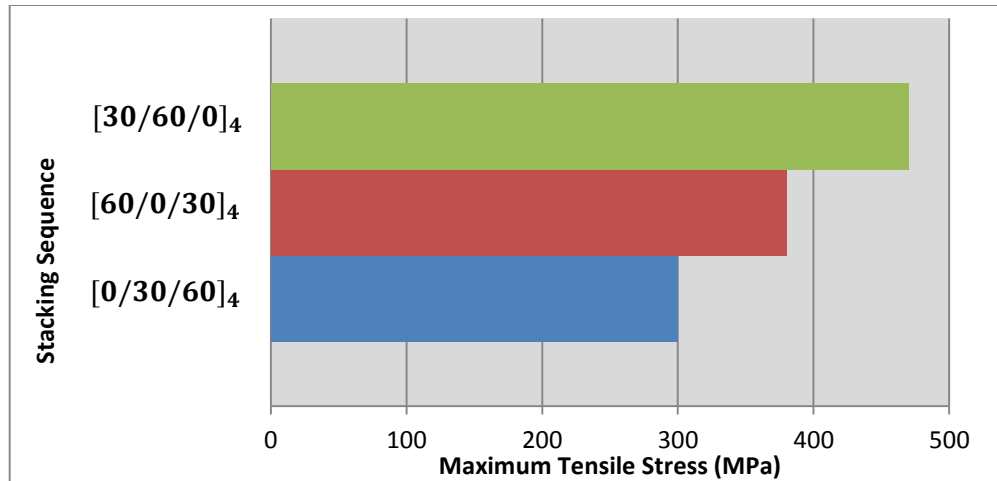


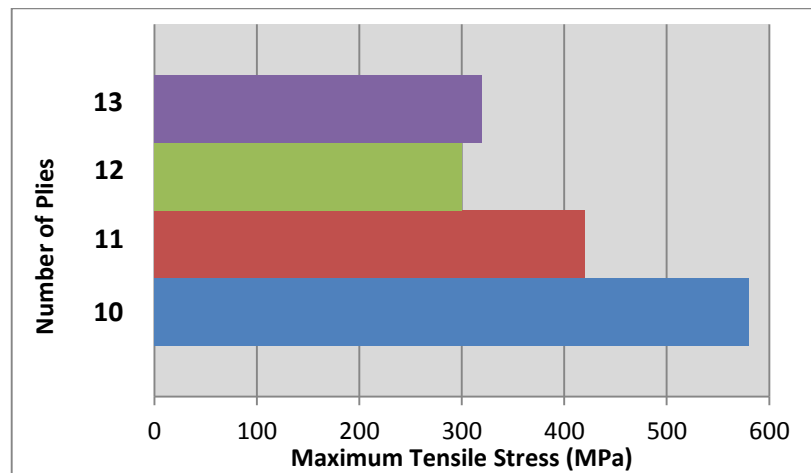
Figure 2.5: The effect of different stacking sequence with a fixed ply number [13]

There were four specimens of different ply number for each LSS. It was observed that for laminate with 11 plies number, the effective elastic modulus in x-axis for stacking sequence of [0/30/60] is 253.8 GPa, while for stacking sequence of [30/60/0] the effective elastic modulus obtained is 233.9 GPa [13]. The same trend was also observed for ply number 10 and 13. However, the effective modulus is not sensitive to the ply number 12 even with difference of LSS. The reason is probably that 12 is a good number of integer multiplier for the plies with [0/30/60] layup. For that reason, Zhao *et al.* [13] concluded that the right number of plies must be chosen for a given layup.

Furthermore, LSS orientation also might affect the maximum tensile stress. Figure 2.6 shows two set of results with different situation. Figure 2.6 (a) illustrates that the same number of ply with different LSS orientation would result in various maximum tensile stress obtained. Meanwhile, Figure 2.6 (b) shows the maximum tensile stress for the same LSS orientation of [0/30/60] with different ply number.



(a)



(b)

Figure 2.6: (a) Maximum tensile stress for different LSS orientation with the same ply number, (b) Maximum tensile stress for different ply number with the same LSS orientation of [0/30/60] [13]

Moreover, the fracture toughness also might be affected by the LSS as shown in Figure 2.7. The materials used for this experiment was carbon fiber with epoxy as the matrix. Each LSS was constructed with a symmetrical 4 plies and being tested for the failure load by conducting the tensile test. The highest failure load was shown by LSS with 15° orientation which could withstand 6516 N of load while 90° orientation is the lowest with 3680 N [14]. From the results, the failure loads tends to decrease with the increase of fiber orientation. Meanwhile, Houshyar *et al.* [7] also showed the same trend of results as in Figure 2.8.

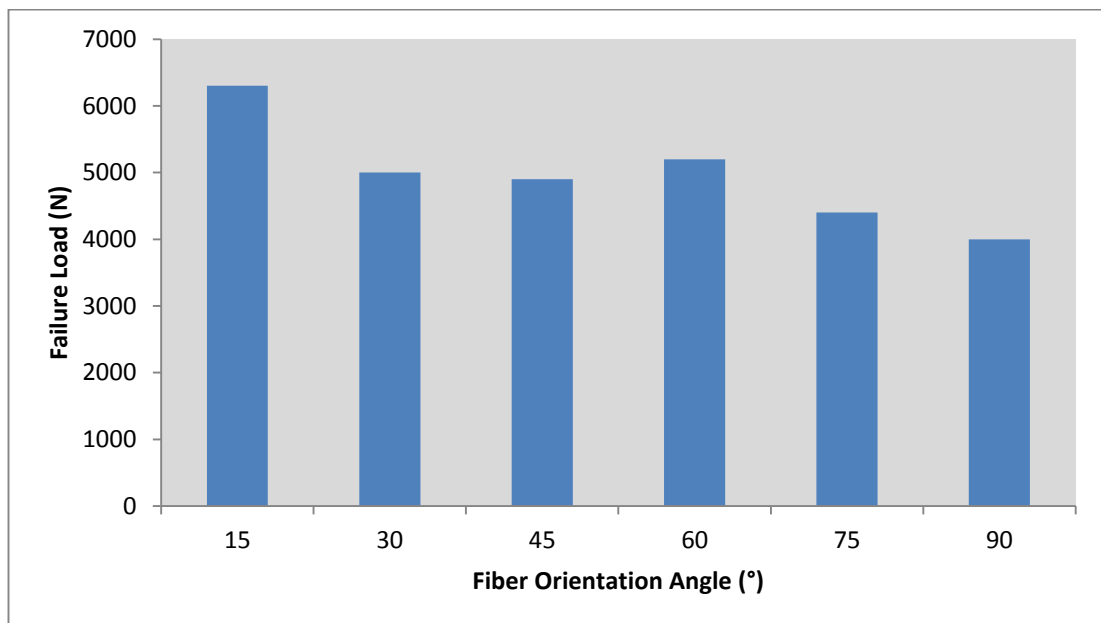


Figure 2.7: Variation of failure loads with fiber orientation angle [14]

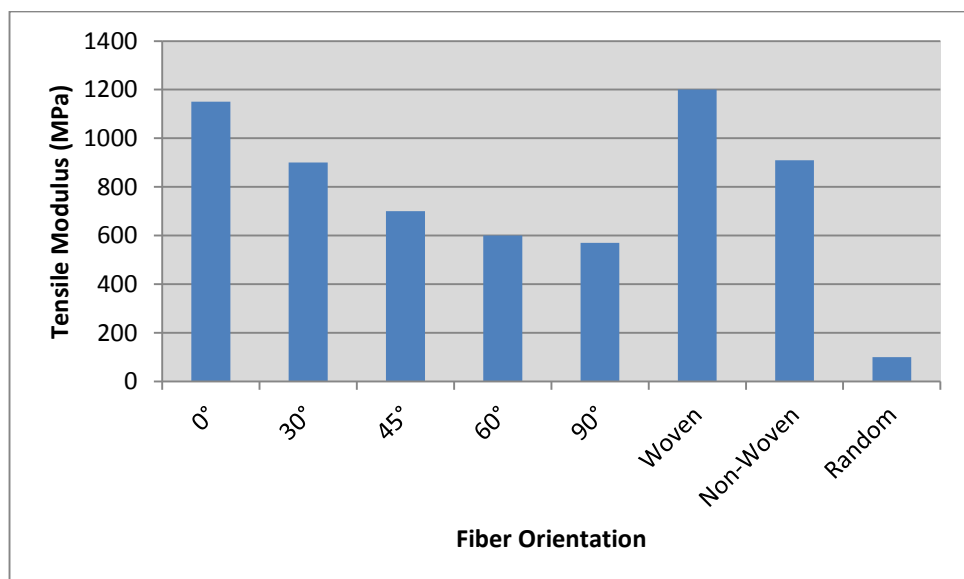


Figure 2.8: Variation of tensile modulus with fiber orientation angle [7]

Another study had been conducted by Subagia *et al.* [2] to investigate the properties of two different composite materials, which are basalt fiber and carbon fiber. This study was conducted with a fixed 10 number of plies. Nine samples consisted with several combinations of carbon/basalt fibers and layup sequences as shown in Figure 2.9 had been tested for their flexural strength with three-point bending test. Referring to the result in Figure 2.10, various values of flexural properties were obtained for all the samples. The highest flexural strength and modulus was shown by carbon fiber, while the lowest was shown by basalt fiber. Eventhough these two materials show different flexural results, it was clearly shown that by changing the layup sequences (in this case by having hybrid composite) the flexural strength and flexural modulus are affected. These results proved that the properties of the laminate are dependent on the layup sequences of the composite.

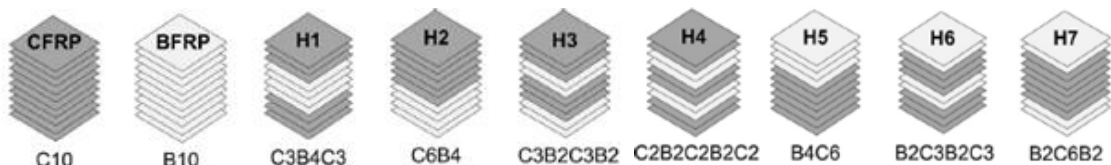


Figure 2.9: Different stacking sequences of carbon (C) and basalt (B) fiber plies [2]

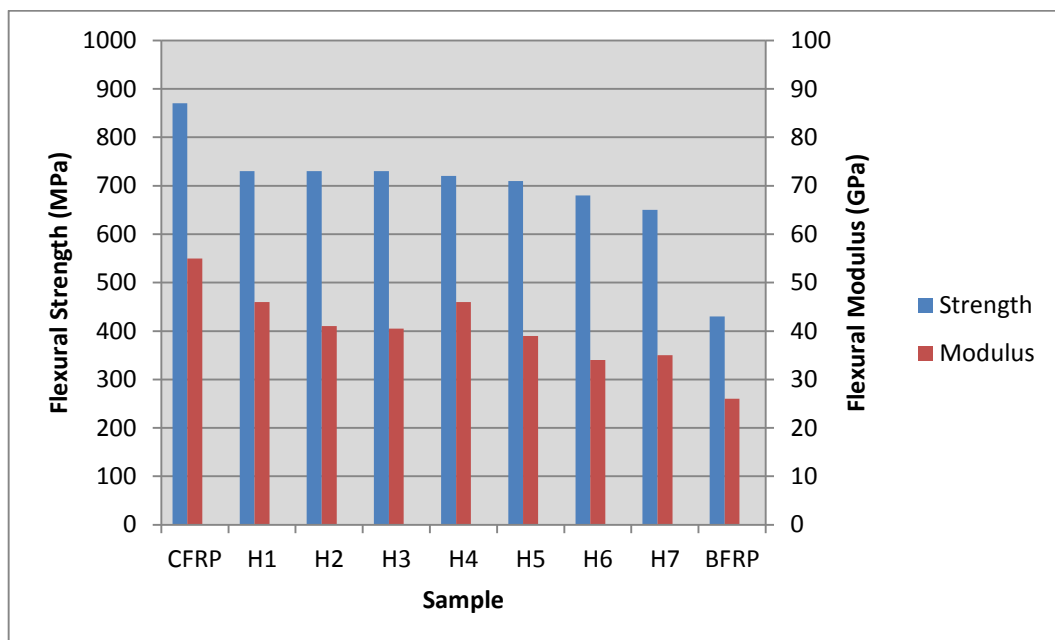


Figure 2.10: Average flexural strength and modulus of CFRP, BFRP and interply hybrid composites with different stacking sequences [2]

CHAPTER 3

METHODOLOGY

3.1 Project Flow Chart

The overall steps for conducting the project are illustrated in Figure 3.1 below.

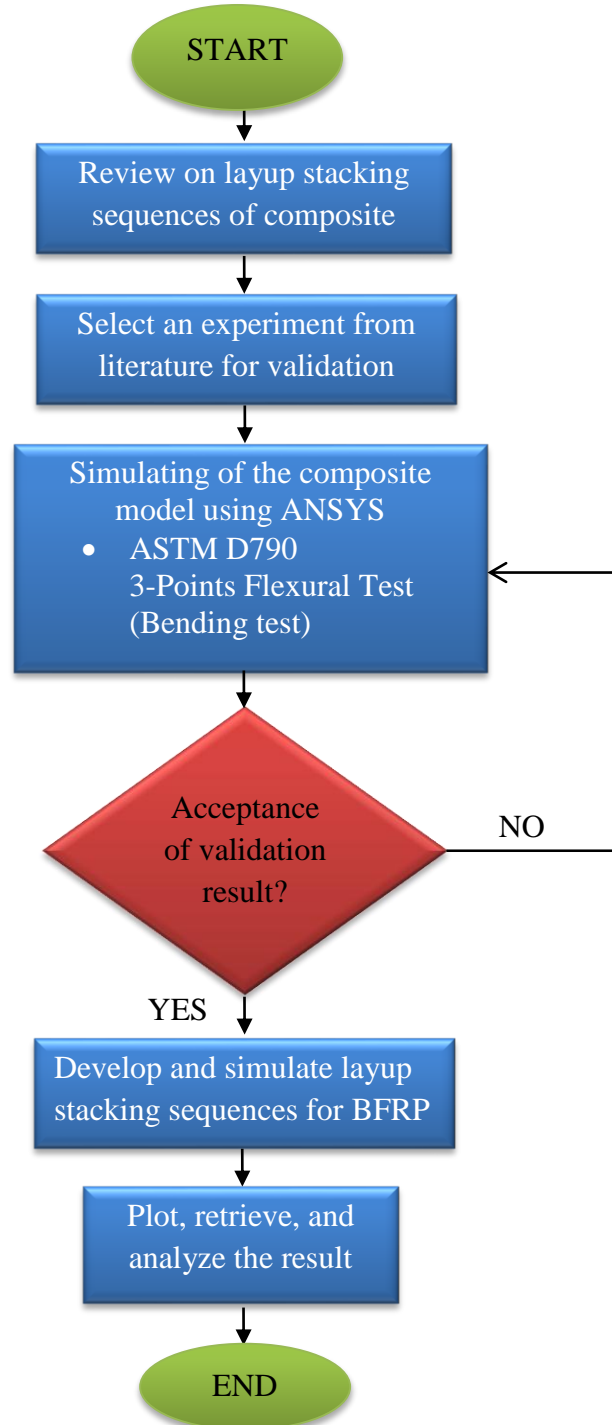


Figure 3.1: Flow of the project

3.2 Composite Material Properties

The analyzed material for the simulation was assumed as isotropic with 100% volume of fiber. Carbon fiber and glass fiber were used for validation and benchmark purposes, while basalt fiber was used as the main material for LSS design. Table 3.1 shows the materials properties for pre-impregnated fibers with epoxy used for the validation purpose.

Table 3.1: Properties for the materials [15]

Properties		Material		
		Basalt/Epoxy	Glass/Epoxy	Carbon/Epoxy
Young's Modulus (MPa)	X	37700	29700	121000
	Y	5237	4000	8600
	Z	5237	4000	8600
Poisson's Ratio	XY	0.2	0.22	0.27
	YZ	0.21	0.23	0.4
	XZ	0.21	0.23	0.27
Shear Modulus (MPa)	XY	2050	2070	4700
	YZ	3630	3070	3100
	XZ	3630	3070	4700

3.3 FEA Procedures for Result Validation

At the end of this project, an optimum design of LSS will be established for BFRP by selecting the best strength and stiffness composite. Several steps are required to be followed in order to achieve the desired results. This is important to ensure that the project is successful. First of all, some knowledge on composite and engineering materials are needed to understand the problem statements and the objectives by reading and analyzing the literature review. Second step is modeling and simulation. For this part, data and properties of BFRP must be correctly gathered and keyed in the ANSYS software for simulation process. The second step will start by the selection of a previous experiment from literature for validation purpose. For the simulation, an experiment set up by Subagia *et al.* [2] was considered. This experiment was selected due to its feasibility, and also the availability of orthotropic

materials properties for carbon fiber. The materials properties needed for composite simulation must be in 3 directions (orthotropic) [16]. The main focus for the validation is to ensure that FEA simulation will produce the same results as the experiment done in the literature. A three-point flexural test was simulated according to ASTM D790. The dimension of the carbon fiber composite is as shown in Figure 3.2.

Table 3.2: Dimensions for Carbon/Epoxy composite

Properties	Dimension
Length	76.2 mm
Width	12.7 mm
Thickness of Composite	2.3 mm
Span Length	73.6 mm
Number of layers	10 layers
Span-to-depth ratio	32

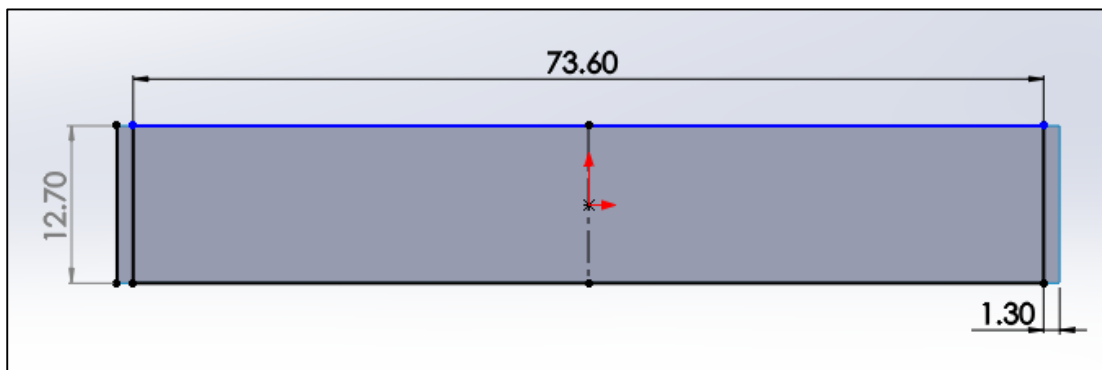


Figure 3.2: Dimension (in mm) of the carbon/epoxy composite

A composite with ten layers of carbon/epoxy was created using ANSYS composite pre-post (ACP). The simulation was done under static structural stand-alone analysis as shown in Figure 3.3. The mesh was generated for the specimen as shown in Figure 3.6. Two simple supports were applied to represent the span supports as in Figure 3.8. After that, a range of load from 100 N to 1000 N was applied on the composite in Y-direction, Figure 3.10. The results of the simulation are shown in Figure 3.12. Then, the simulation result obtained was compared and analyzed with the experimental result from literature as in Table 4.1, and Figure 4.1. Step by step procedure is described in the following pages.

1. Selection of analysis. Static structural analysis as in Figure 3.3 was selected for flexural test simulation.

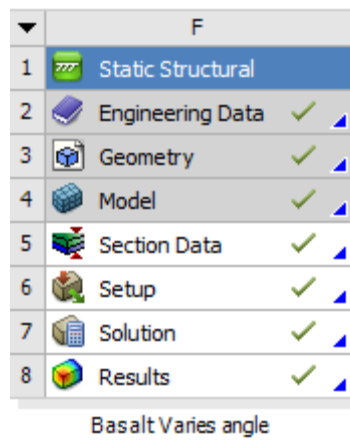


Figure 3.3: Static structural stand-alone analysis

2. Materials properties for all the fibers were inserted into engineering data, refer to Figure 3.4.

Outline of Schematic A2, B2: Engineering Data				
	A	B	C	D
1	Contents of Engineering Data	Source	Description	
2	Material			
3	Basalt Fiber			
4	Carbon Fiber			
5	Epoxy			
6	Glass Fiber			
*	Click here to add a new material			

Properties of Outline Row 3: Basalt Fiber					
	A	B	C	D	E
1	Property	Value	Unit		
2	Density	2700	kg m ⁻³		
3	Isotropic Elasticity				
9	Orthotropic Elasticity				
10	Young's Modulus X direction	3.77E+10	Pa		
11	Young's Modulus Y direction	5.237E+09	Pa		
12	Young's Modulus Z direction	5.237E+09	Pa		
13	Poisson's Ratio XY	0.2			
14	Poisson's Ratio YZ	0.21			
15	Poisson's Ratio XZ	0.21			
16	Shear Modulus XY	2.05E+09	Pa		
17	Shear Modulus YZ	3.63E+09	Pa		
18	Shear Modulus XZ	3.63E+09	Pa		
19	Bilinear Isotropic Hardening				
20	Yield Strength	300	MPa		
21	Tangent Modulus	1000	MPa		

Figure 3.4: ANSYS engineering data for defining materials properties

3. Figure 3.5 shows the plane model of the composite which was designed using SOLIDWORK and imported into the ANSYS.

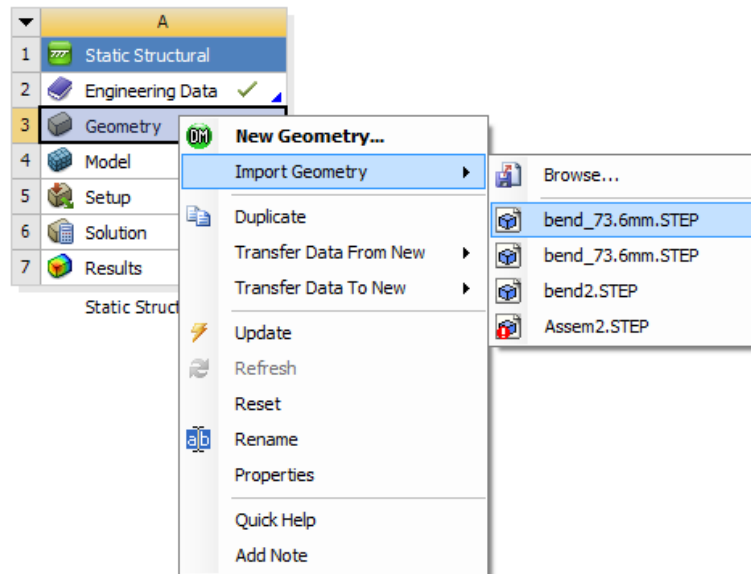


Figure 3.5: Importing the composite geometry

4. The imported geometry was meshed with program controlled sizing as shown in Figure 3.6.

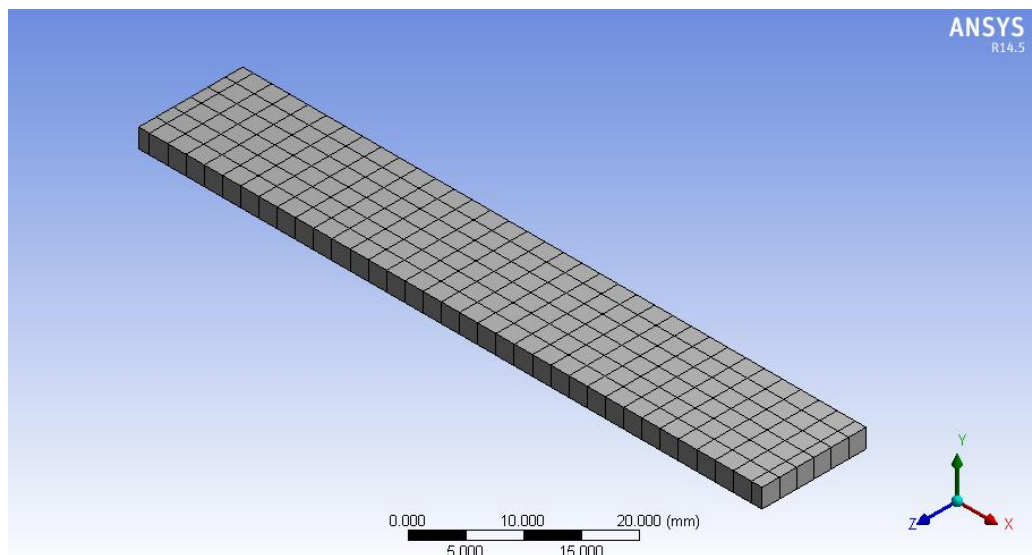


Figure 3.6: Meshing of the composite

5. Simple supports were applied on 2 lines (blue color), refer to Figure 3.7.

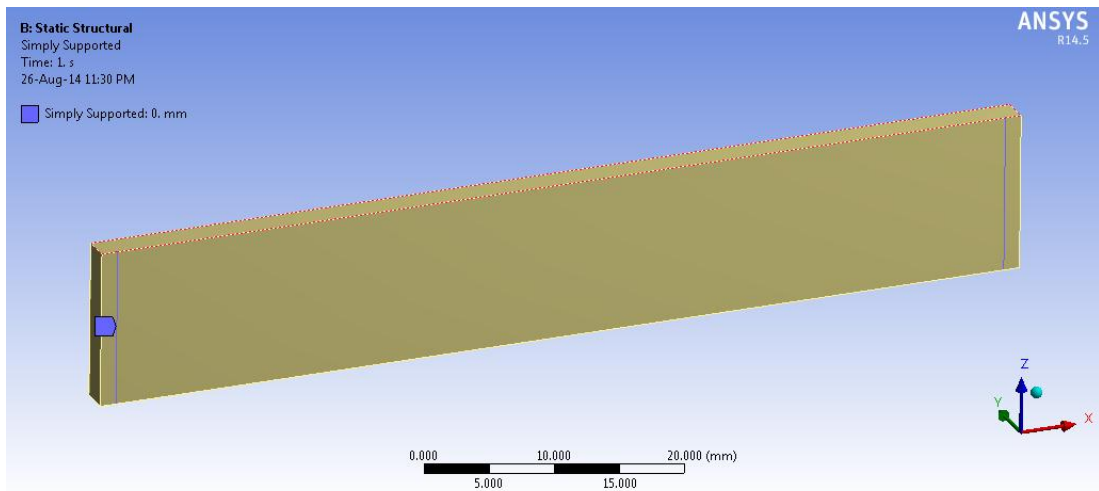


Figure 3.7: Simple support applied (blue color)

6. The number of steps were set up to 10 steps as shown in Figure 3.8 with large deflection option was on and iterative solver selected.

[-] Step Controls	
Number Of Steps	10.
Current Step Number	1.
Step End Time	1. s
Auto Time Stepping	Program Controlled
[-] Solver Controls	
Solver Type	Iterative
Weak Springs	Program Controlled
Large Deflection	On
Inertia Relief	Off
[+] Restart Controls	
[+] Nonlinear Controls	
[+] Output Controls	
[+] Analysis Data Management	
[+] Visibility	

Figure 3.8: Steps control setting

7. Then, a range of force from 0-1000 N was applied on the composite surface as in Figure 3.9 and Figure 3.10.

	Steps	Time [s]	Force [N]
1	1	0.	0.
2	1	1.	100.
3	2	2.	200.
4	3	3.	300.
5	4	4.	400.
6	5	5.	500.
7	6	6.	600.
8	7	7.	700.
9	8	8.	800.
10	9	9.	900.
11	10	10.	1000.
*			

Figure 3.9: Tabular data for force applied

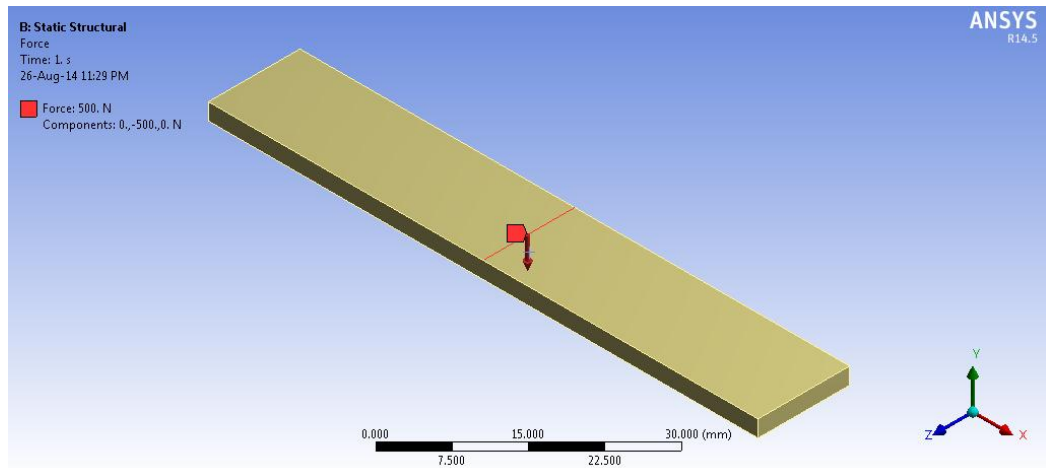


Figure 3.10: Force applied on the composite (red color)

8. Total deformation was selected under solution as the desired output, refer to Figure 3.11.

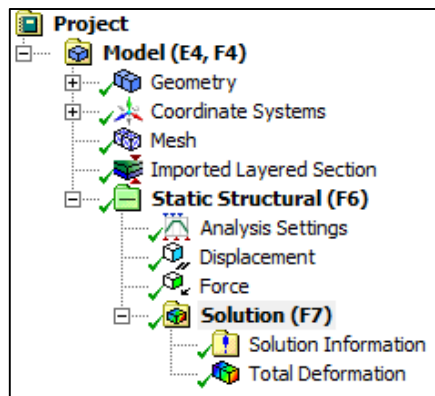


Figure 3.11: Inserting total deformation under solution branch

9. Run the simulation and the desired result selected will be plotted as shown in Figure 3.12.

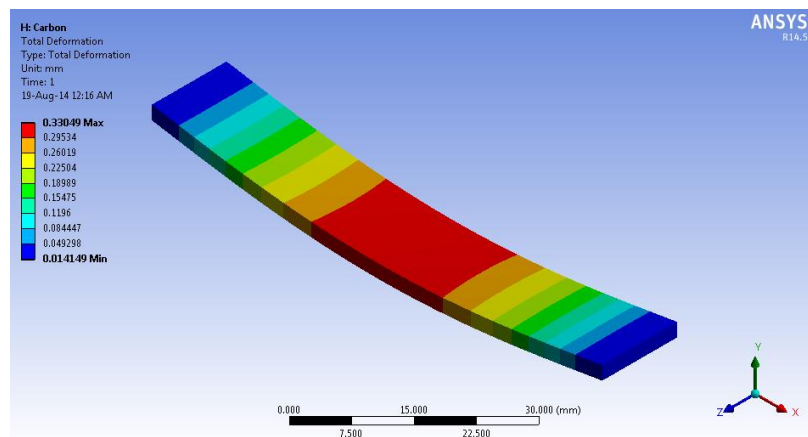


Figure 3.12: Example of the simulation result on the composite

3.4 FEA Procedures for Designing Layup Stacking Sequences

After the simulation was validated with acceptable results compared with the literature results, the layup stacking sequence could now be designed on basalt fiber reinforced composite. All the steps considered are mostly the same steps as being done during validation, where the only changes are on the properties of the material and also the introduction of the angle orientation of the fiber for each layer. For benchmarking purpose, three types of material which are basalt fiber, glass fiber and also carbon fiber were simulated with the same layup stacking sequence in order to study the strength of these three materials. All the properties are as shown earlier in Table 3.1. Ten layers of 0° angle of fiber was introduced for each material.

The results for these three materials were compared as a benchmark to overview the strength of the basalt fiber with carbon fiber and glass fiber when subjected to ten layers of 0° fiber orientation. The results were collected and discussed later on the next chapter. Then the next step is to proceed with designing of different models of BFRP with varying angles of stacking sequences. The results for the basalt fiber with ten layers of 0° fiber orientation was taken as the benchmark in designing the stacking sequences and labeled as sample 1 (S1). There were 12 samples of BFRP with different layup stacking sequences designed and categorized into alternate, alternate symmetrical and random symmetrical. Table 3.3 shows the summary of the layup stacking sequences for all the samples.

The same 3-point flexural test simulation was done for all the samples, and the entire boundary conditions were applied according to the steps taken during the validation process. The fiber orientation was introduced inside ANSYS composite pre-post (ACP), where each layer will be predefined with the desired angle orientation. The 0° angles of the fiber was set to be parallel with the composite length, and every incremental of angle will follow clockwise direction as shown in Figure 3.16 until Figure 3.20. All the samples were simulated with the same range of load between 100 N until 1000 N, then the deflection result was plotted inside ANSYS and being compared and further analyzed. Step by step procedure for designing the LSS and fiber orientation is described in the following pages.

Table 3.3: Layup stacking sequences for each sample

Sample	Fiber Type	Stacking Sequence	Design Category
S1	Basalt Fiber	$[0]_{10}$	Default/Benchmark
S2	Basalt Fiber	$[0/45/0/45/0]_S$	Alternate Symmetrical
S3	Basalt Fiber	$[0/60/0/60/0]_S$	
S4	Basalt Fiber	$[0/90/0/90/0]_S$	
S5	Basalt Fiber	$[0/45]_5$	Alternate
S6	Basalt Fiber	$[0/60]_5$	
S7	Basalt Fiber	$[0/90]_5$	
S8	Basalt Fiber	$[45/0/0/0/0]_S$	Random Symmetrical
S9	Basalt Fiber	$[60/0/0/0/0]_S$	
S10	Basalt Fiber	$[0/45/90/0/60]_S$	
S11	Basalt Fiber	$[45/0/0/90/60]_S$	
S12	Basalt Fiber	$[0/0/45/0/0]_S$	

1. Figure 3.3 shows ANSYS Composite Pre-Post stand-alone analysis was linked with static structural stand-alone analysis.

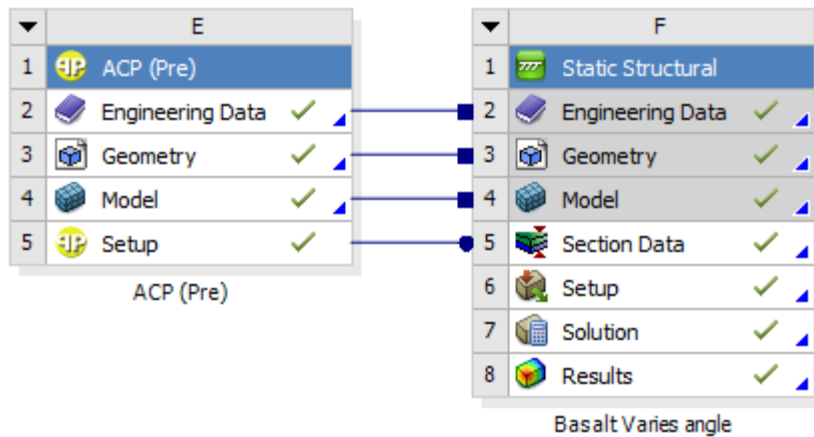


Figure 3.13: Static structural stand-alone analysis with ANSYS Composite Pre-Processing (ACP)

2. The fabric thickness and stackup sequences were defined inside ANSYS ACP setup. Ten layers of fabrics were designed with a thickness of 0.23 mm for each layer. Refer to Figure 3.14 and Figure 3.15.

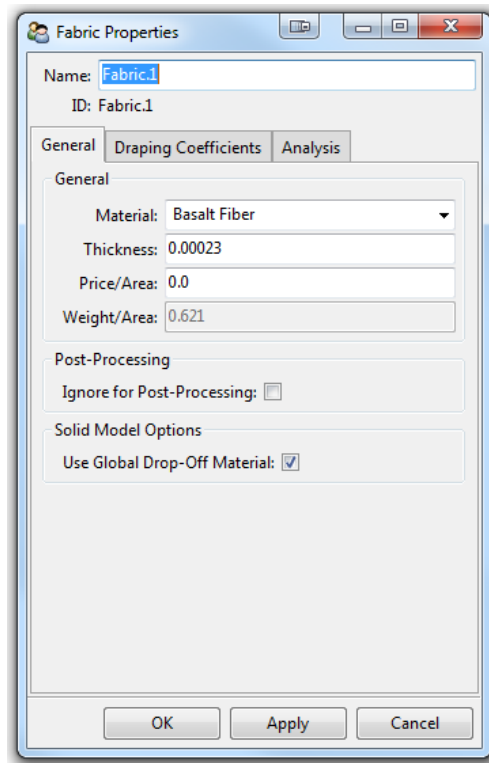


Figure 3.14: ANSYS composite pre-post (ACP) setting for layer thickness

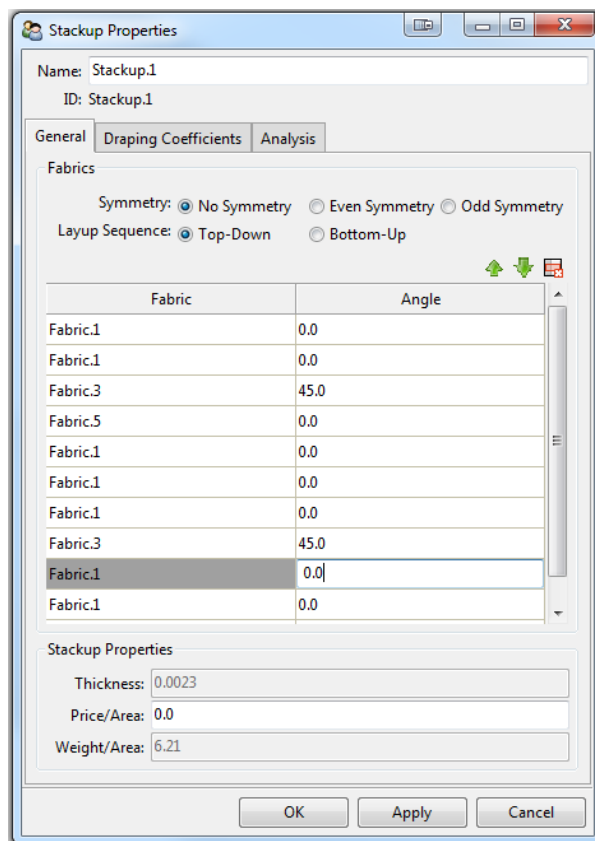


Figure 3.15: ANSYS composite pre-post (ACP) setting for fiber orientation

3. Then, the number of layers for the composite will be automatically generated according to the defined thickness and angle orientation as shown in Figure 3.16.

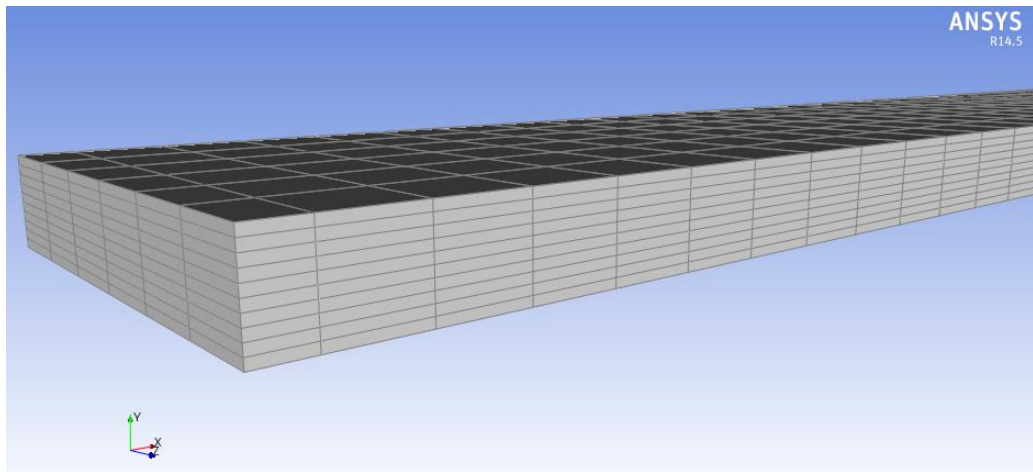


Figure 3.16: Layers of the composite

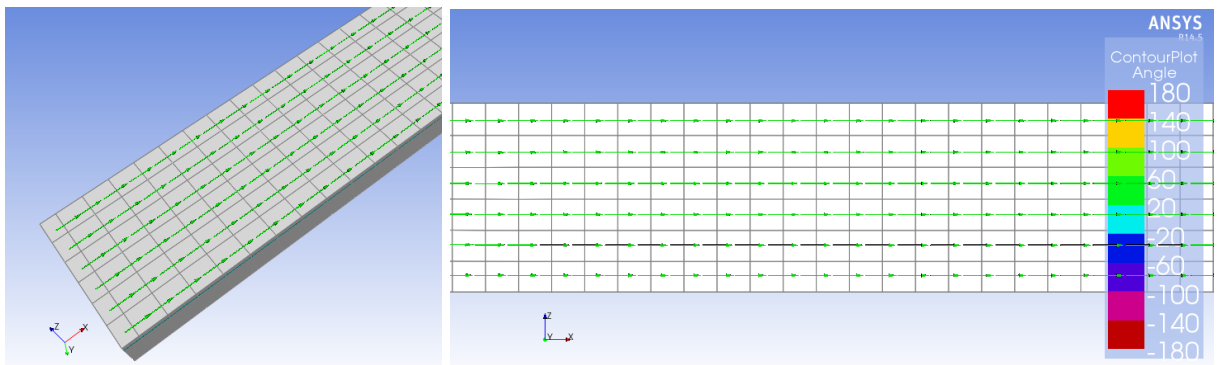


Figure 3.17: 0° fiber orientation

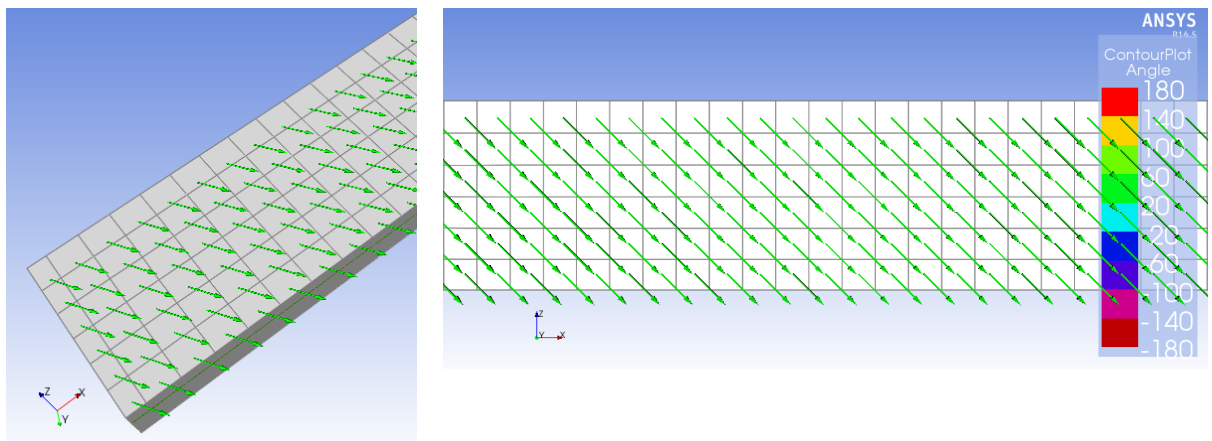


Figure 3.18: 45° fiber orientation

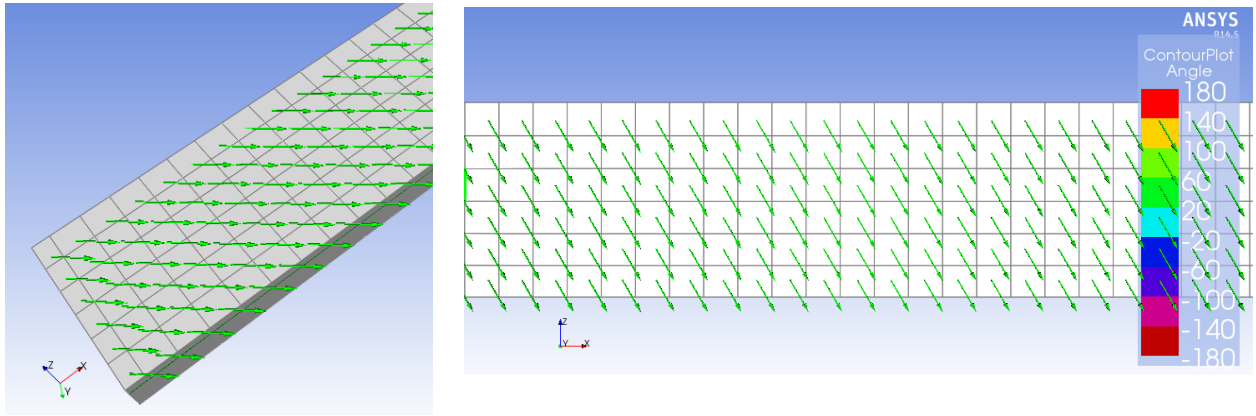


Figure 3.19: 60° fiber orientation

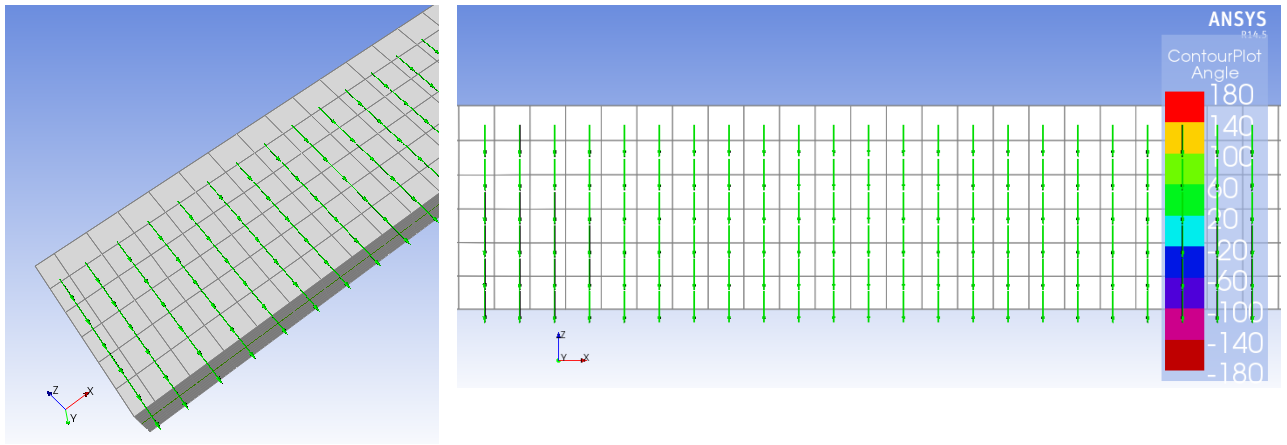


Figure 3.20: 90° fiber orientation

4. After defining the LSS and fiber orientation, then repeat all the steps taken on Section 3.3 to apply the boundary conditions.

3.5 Progress Summary and Milestone

Project Gantt chart and key milestones shown in Table 3.4 and Table 3.5 for FYP 1 and FYP 2 respectively were established in order to ensure the smoothness of the project activities.

Table 3.4: Gantt chart, milestones and project activities for FYP1

No.	Activity/Week	Comment	Submission/ Dateline	1	2	3	4	5	6	7	8	9	10	11	12	13	14
1	FYP1 first briefing	Done	15/1/2014	■	■												
2	Project selection	Done	23/1/2014	■	■												
3	First meeting with supervisor	Done	27/1/2014			■											
4	FYP1 second briefing	Done	29/1/2014			■											
5	Literature review	Read 30 journals/articles	-			■	■	■	■								
6	Field trip to SIRIM Shah Alam	Wood polymer composite	11/2/2014					■									
7	Working on the extended proposal	Done	23/3/2014					■									
8	First draft of extended proposal	Need review from SV - Done	△						■								
9	Submission of extended proposal	Done	23/2/2014						■								
10	Literature review continuation	Done							■	■	■	■					
11	ANSYS training	Hands on training	△						■	■	■						
12	Proposal defense	Done	△								■	■					
13	Validation of results	Find one experiment and validate the result using ANSYS	△								■	■	■	■	■	■	■
14	Working on the interim report	Done												■	■		
15	First draft of interim report	Need review from SV	△													■	
16	Submission of interim report	Done	20/4/2014														■

*Note = Milestones are indicate with “△” symbol on the Gantt chart.

Table 3.5: Gantt chart, milestones and project activities for FYP2

No.	Activity/Week	Comment	Submission/ Dateline	1	2	3	4	5	6	7	8	9	10	11	12	13	14
1	First meeting with supervisor	Done	22/5/2014	■													
2	Validation for non-linear result	Done	△	■	■	■											
3	Obtaining orthotropic material properties for basalt and glass fiber	Taken from PHD student	3/6/2014				■										
4	Discussion on non-linear simulation	Discussion with SV and PHD student	△					■	■								
5	Design and simulation on layup stacking sequences for BFRP	Design several layup and orientation	△					■	■	■	■						
6	Working on the progress report	Done	6/7/2014							■	■						
7	Submission of progress report	Done	6/7/2014								■						
8	Pre-SEDEX poster and presentation	Prepare a poster	△									■	■				
9	Submission of dissertation draft to supervisor		10/8/2014												■		
10	Submission of technical paper		△													■	
11	Oral presentation (VIVA)		△														■
12	Submission of dissertation	Hard bound copy	△														■

*Note = Milestones are indicate with “△” symbol on the Gantt chart.

CHAPTER 4

RESULTS AND DISCUSSION

4.1 Results Validation with Carbon Fiber

The validation results were obtained from a nonlinear simulation of carbon fiber reinforced composite (CFRP). Figure 4.1 shows the plotted load versus displacement graph by comparing the results from ANSYS and literature. It could be clearly seen that the results from ANSYS and the literature agree well in the elastic region where both of the lines were overlapped. In the plastic region, the literature results show that the CFRP would fail at 800 N meanwhile there was no failure shown for ANSYS result. This is one of the disadvantages of the ANSYS where the failure criterion has to be defined accordingly. Assumption made for the simulation was that the composite is in perfect condition with 100% fiber volume, this might be the reason why the lines in plastic region were not overlapped, and the values obtained were slightly different in this region. Other reason that could affect the ANSYS results might be the properties of carbon fiber. The simulation was done by using the default orthotropic properties of carbon from ANSYS which possibly might be different from the real properties of carbon fiber used by the literature.

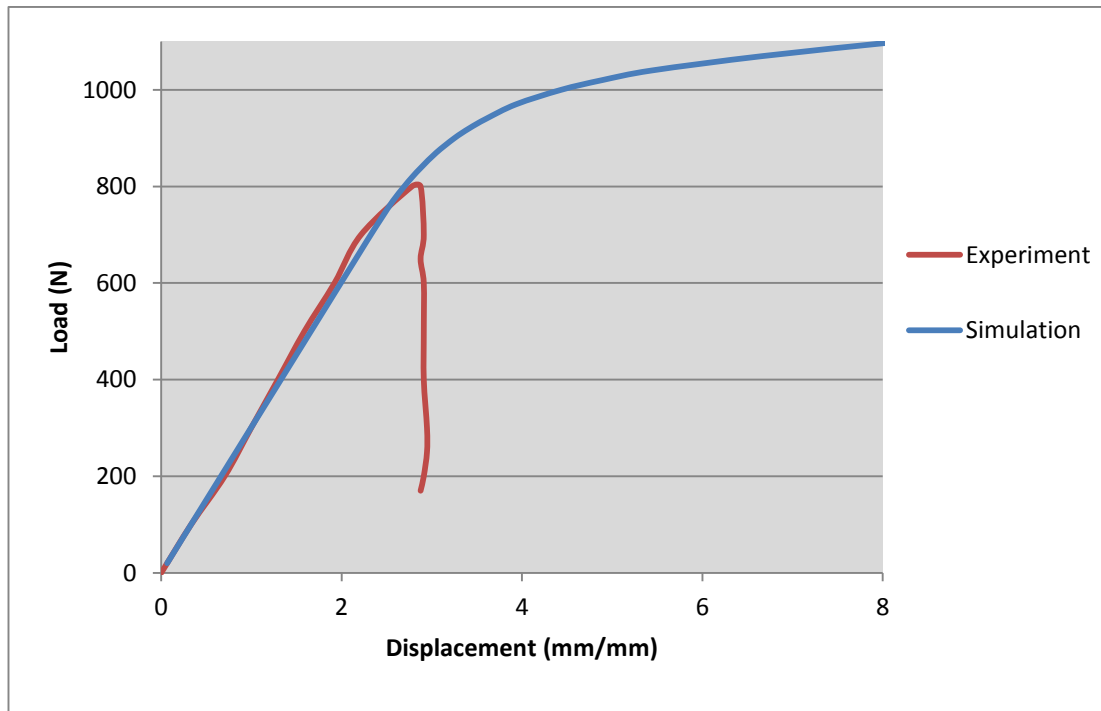


Figure 4.1: Load versus displacement graph for result validation

Looking at the graph for ANSYS results, the line would become less steep after 800 N, and this behavior could be considered as the failure point of the CFRP in ANSYS. Therefore the highest load that the fiber could withstand is around 850 N where the value is taken just before the graph became flat. Table 4.1 and Figure 4.2 show the comparison of the results up to 800 N, where the real CFRP from the literature would break.

Table 4.1: Results comparison

Load (N)	Displacement (mm) (simulation)	Displacement (mm) (experiment)
0	0	0
100	0.33098	0.331646
200	0.63242	0.703797
300	0.95467	0.997468
400	1.327	1.29367
500	1.6593	1.58734
600	1.9914	1.92152
700	2.3356	2.21519
800	2.8291	2.77975
900	3.8863	-
1000	7.7712	-

4.2 Benchmarking of Results

The purpose of result benchmarking is to compare the strength of the BFRP with GFRP and CFRP when subjected to the same fiber orientations with ten layers. The fiber orientations were set as 0° for all the layers of each composite. The results obtained are as shown in Figure 4.2. From the figure, CFRP shows the steepest behavior and rapid load rise among the other two composites. Besides, it also shows a low displacement behavior, indicating a brittle property. On the other hand, GFRP shows a contrary behavior with a slow load rise, largest yield displacement and lowest maximum load among the three samples. This is suggesting that GFRP has a good ductility primarily due to the high elongation of glass fiber. Meanwhile, BFRP results fall in the middle of the CFRP and GFRP. Thus, it could be concluded that basalt fiber would have a better ductility than carbon fiber and also a better strength than glass fiber which agrees with the finding from Manikandan *et al.* [17].

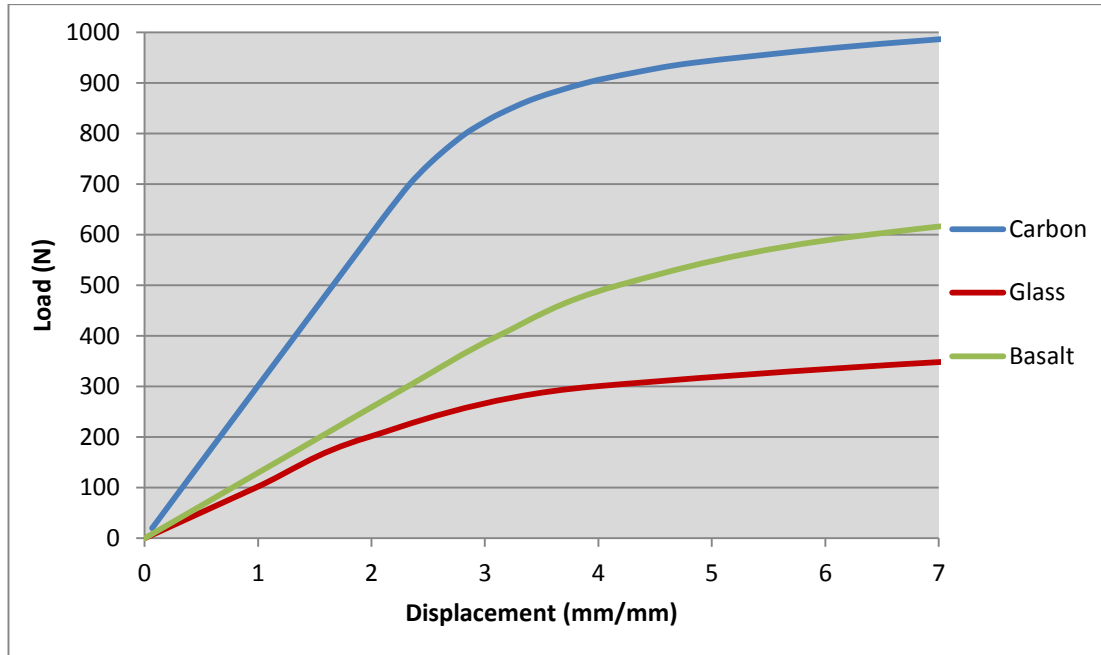


Figure 4.2: Load versus displacement comparison for BFRP, GFRP and CFRP

The load and deformation obtained from ANSYS were used to calculate the flexural stress and flexural strain for the three composites. Then, the stress-strain curves were plotted in order to further study the behavior of the composites. Below are the two formulas being used to calculate the stress and strain according to ASTM D790 standard [18].

$$\sigma_f = 3PL/2bd^2 \quad (1)$$

where:

σ_f = stress in the outer fibers at midpoint, MPa

P = load applied, N

L = support span length, mm

b = width of the composite, mm

d = depth/thickness of the composite, mm

$$\varepsilon_f = 6Dd/L^2 \quad (2)$$

where:

ε_f = strain at outer surface, mm/mm

D = maximum deflection at the center of the composite, mm

d = depth/thickness of the composite, mm

L = support span length, mm

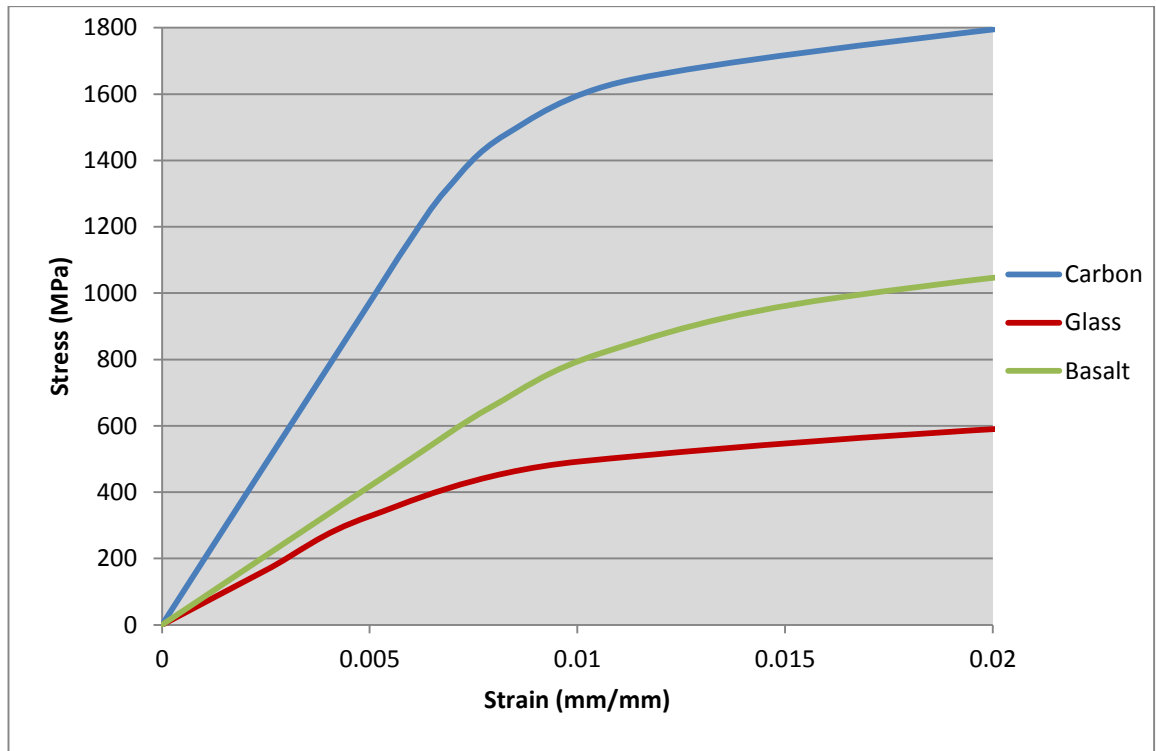


Figure 4.3: Stress-strain curve for BFRP, GFRP and CFRP

Figure 4.3 shows the stress-strain curve for all the three materials. By comparing Figure 4.2 and Figure 4.3, the patterns of the lines for both of the figures are the same since the stress-strain are derived from the load-deformation, and it is following the two formulas considered. From both of the formulas, all the values are kept constant except for applied load and the deformation. Therefore, the pattern of the graph obtained will be the same. From Figure 4.3, BFRP still falls in between GFRP and CFRP with a maximum stress value at 850 MPa. This behavior of BFRP will be used as a benchmark in designing several layup stacking sequences of BFRP.

4.3 Results for Layup Stacking Sequences of BFRP

The layup stacking sequences considered could be grouped into three categories depending on the fiber orientations, which are alternate, alternate symmetrical and random symmetrical. These three categories produced a different pattern of results. Based on Figure 4.4, it can be concluded that sample 2 until sample 4 that have alternate symmetrical fiber orientation show a higher load rise and strength compared to alternate fiber orientation. Moreover, this also portrayed that sample 2- 4 are less ductile than the samples with alternate angle.

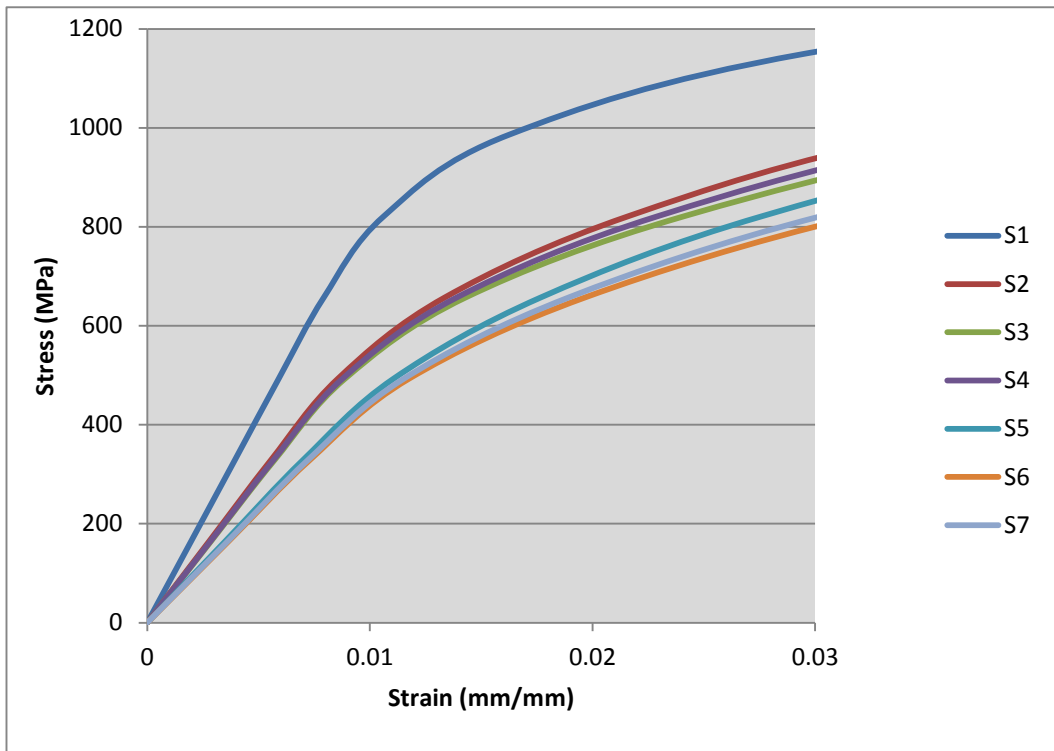


Figure 4.4: Stress-strain curve for alternate and alternate symmetrical fiber orientation.

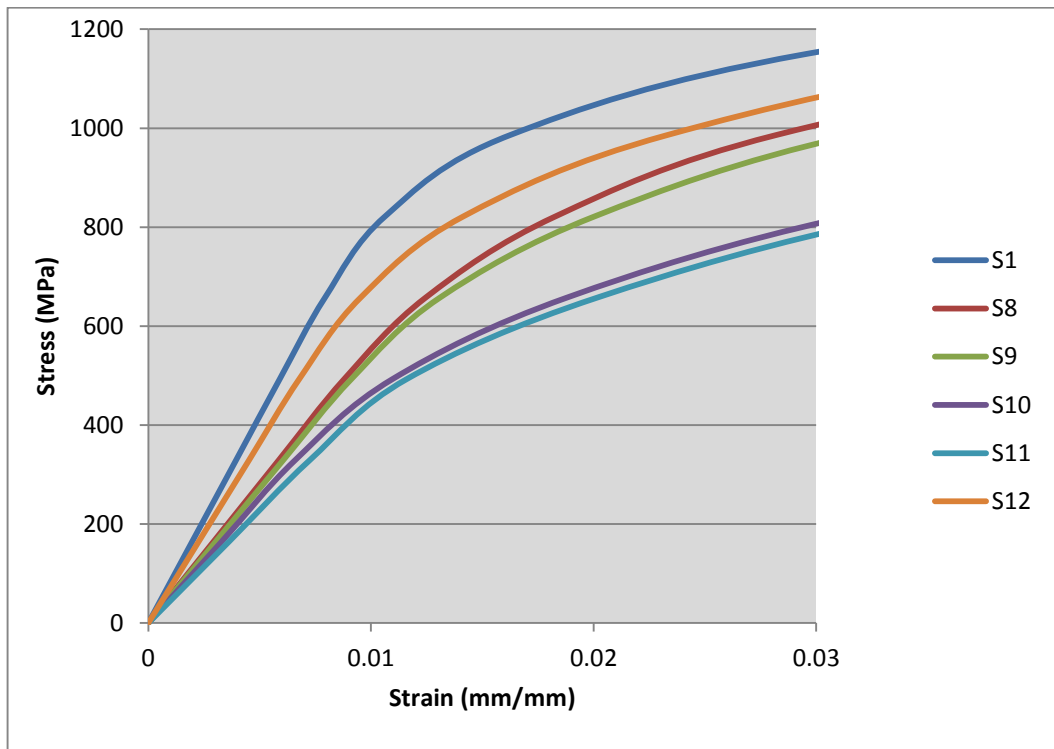


Figure 4.5: Stress-strain curve for random symmetrical fiber orientation

This pattern of results which are in favor of the alternate symmetrical might be due to the presence of more 0° layer compared to the samples with alternate angles. Since sample 1 acts as the benchmark, it could be seen that this sample shows the highest strength among the others since this sample consisted of ten layers of 0° fiber orientation. The simulation were done by simulating 3-point flexural test, therefore 0° layer might withstand more load than other angle orientation since the direction is parallel and along with the fiber direction. This finding is similar with the results shown by several papers where the sample with 0° layer portrayed the highest mechanical properties [7,14,19]. For alternate symmetrical samples, there are six layers of 0° fiber orientation while only five for alternate samples. This clarifies why the results for alternate symmetrical are better than alternate samples. The presences of other angle orientation (45° , 60° and 90°) for sample 2 until sample 7 do not make much differences on the results obtained since 0° layers are still dominating the results.

Referring to Figure 4.5 for random symmetry results, sample 12 shows the highest strength among all 12 samples due to its design with eight layers of 0° fiber orientation and two layers of 45° fiber orientation. Sample 8 also consisted with the same number of layers and fiber orientation as sample 12, but it shows a lower strength than sample 12. This is due to the different position of the two layers of 45° fiber orientation on both samples. For sample 12, the 45° layers were positioned on third and eighth layer, while for sample 8 the 45° layers were on the first and the last layer. In a nutshell, the positions of the 45° layers on both samples are crucial in determining the strength of the BFRP.

By changing the first and the last layer of sample 8 with 60° fiber orientations, resulted with a lower strength of the composite as shown for sample 9. Meanwhile, sample 10 and sample 11 are comprised of all three angles of fiber orientation but with different stacking sequences. Because of that, sample 11 exhibits a better strength as compared to sample 10. From all the results obtained, the difference in fiber orientation and stacking sequences could make a huge difference on the strength of the BFRP. Refer to appendices for complete data of load/deflection and stress/strain for all the samples.

CHAPTER 5

CONCLUSION AND RECOMMENDATION

In a nutshell, it is important to investigate the effect of fiber orientation and layup stacking sequences on the BFRP since it is a newcomer in the composite field. By having a simulation of different fiber orientation, the results obtained could be used to predict the strength and behavior of the BFRP. The results of simulation for 3-points flexural test shown that the 0° layer is the main and dominant factor that determine the strength of the composite. The highest strength was shown by sample 1 with ten layers of 0° fiber orientations, followed by sample 12 which comprised of ten random symmetry of angles, $[0/0/45/0/0]_S$. These findings could be used to determine the suitable applications of BFRP with respect to different fiber orientation and stacking sequences. Therefore, the optimum and the best strength and behavior could be designed to suit with the applications.

There are many more design that could be done on the BFRP, such as by having more than ten layers with respect to different fiber orientation and stacking sequences. As for this project, the layers are fixed to 10 layers for ease of simulation and result interpretations. Since the results showed that 0° layer is the dominant factor, it could be concluded that this layer behave as isotropic with a 3-point flexural test. In real applications, the composite is expected to withstand load or force not only from a single direction, therefore it is crucial to have a composite comprised with anisotropic behavior. According to Soden *et al.* [20], by introduction of other fiber orientation such as 30° , 50° , 70° and 80° might help to broaden the analysis of the results and also many variations of strength could be chosen to suit with applications. Therefore, it is recommended to perform the simulation on the quasi-isotropic laminates of basalt fiber reinforced composite with biaxial loading.

REFERENCES

- [1] Michael W. Hyer, *Stress Analysis of Fiber-Reinforced Composites Materials*. United States of America: McGraw-Hill, 1998.
- [2] Ary Subagia I.D.G, Yonjing Kim, Leonard D. Tijing, Cheol Sang Kim, and Ho Kyong Shon, "Effect of stacking sequence on the flexural properties of hybrid composites reinforced with carbon and basalt fibers," *Composites: Part B*, pp. 251-258, 2014.
- [3] Lopresto V, Leone C, and De Iorio I, "Mechanical characterisation of basalt fibre reinforced plastic," *Composites: Part B*, pp. 717-723, 2011.
- [4] Edward Archer, S. Buchanan, S. Kirby, and A.T. McIlhagger. (2012, September) University of Ulster. [Online]. <http://eprints.ulster.ac.uk/23258/>
- [5] Colombo C, Vergani L, and Burman M, "Static and fatigue characterisation of new basalt fiber reinforced composites," *Composite Structures*, no. 94, pp. 1165-1174, 2012.
- [6] (2014, August) Creation of the Sea. [Online]. <http://www.creationofthesea.com/wp-content/uploads/2013/05/Black-Basalt-Rock-Faux-Cabinetry.png>
- [7] S. Houshyar, R.A. Shanks, and A. Hodzic, "Effect of Fibre-Orientation on Mechanical Properties of Polypropylene Composites," in *Composites Technologies for 2020*, L. Ye, Y-W. Mai, and Z. Su, Eds. Cambridge, England: Woodhead Publishing, 2004, pp. 41-45.
- [8] Ever J. Barbero, *Introduction to Composite Materials Design*, Second Edition ed. United States of America: CRC Press, 2011.
- [9] Ludwig Burger. (2014, March) Reuters. [Online]. <http://www.reuters.com/article/2014/03/28/sgl-fibres-idUSL5N0MP2RP20140328>
- [10] (2014, August) Alibaba. [Online]. http://www.alibaba.com/trade/search?fsb=y&IndexArea=product_en&CatId=&SearchText=basalt+fiber+
- [11] Yihe Zhang et al., "Mechanical and thermal properties of basalt fiber reinforced poly(butylene succinate) composites," *Materials Chemistry and Physics*, pp. 845-849, 2012.

- [12] Kojiro Morioka and Yoshiyuki Tomita, "Effect of lay-up on mechanical properties and fracture behaviour of CFRP laminate composite," *Materials Characterization*, pp. 125-136, 2000.
- [13] Wei Zhao, Peter K. Liaw, and Niann-i Yu, "Computation of the lamina stacking sequence effect on elastic moduli of a plain-weave Nicalon/SiC laminated composite with a [0/30/60] lay-up," *Journal of Nuclear Materials*, pp. 10-19, 1998.
- [14] Mete Onur Kaman, "Effect of fiber orientation on fracture toughness of laminated composite plates," *Engineering Fracture Mechanics*, vol. 78, pp. 2521-2534, 2011.
- [15] A.N. Mengal, S. Karuppanan, and A.A. Wahab, "Structural analysis of basalt fiber reinforced plastic wind turbine blade," *MATEC*, June 2014.
- [16] E. Madenci and E. Guven, *The Finite Element Method and Application in Engineering Using ANSYS*. New York: Springer, 2007.
- [17] V. Manikandan, J.T. Winowlin Jappes, S.M. Suresh Kumar, and P. Amuthakkannan, "Investigation of the Effect of Surface Modifications on the Mechanical Properties of Basalt Fiber Reinforced Polymer Composites," *Composites: Part B*, pp. 812 - 818, 2012.
- [18] "ASTM Standard D790 - 98," in *Annual Books of ASTM Standards*. West Conshohocken, PA, United States of America: ASTM International, 2009 , ch. Section Eight, pp. 148 - 155.
- [19] H.W. Wang, H.W. Zhou, L.L. Gui, H.W. Ji, and X.C. Zhang, "Analysis of Effect of Fiber Orientation on Young's Modulus for Unidirectional Fiber Reinforced Composites," *Composites: Part B*, pp. 733 - 739, 2014.
- [20] P.D. Soden, M.J Hinton, and A.S. Kaddour, "Lamina Properties, Lay-Up Configurations and Loading Conditions for a Range of Fiber-Reinforced Composite Laminates," *Composites Science and Technology*, pp. 1011-1022, 1998.

APPENDICES

Table A: Simulation data for Sample 1 and Sample 2

Load (N)	Stress (MPa)	Sample 1		Sample 2	
		Deflection (mm)	Strain (mm/mm)	Deflection (mm)	Strain (mm/mm)
0	0	0	0	0	0.186382
100	164.3273	0.77252	0.001968	1.0906	0.186382
200	328.6546	1.545	0.003936	2.1813	0.186382
300	492.9819	2.3176	0.005904	3.3612	0.186382
400	657.3091	3.1135	0.007932	5.2475	0.186382
500	821.6364	4.1738	0.010633	8.4863	0.186382
600	985.9637	6.377	0.016246	13.567	0.186382
700	1150.291	11.617	0.029595	22.261	0.186382
800	1314.618	22.327	0.056879	35.576	0.186382
900	1478.946	38.28	0.097520	52.795	0.186382
1000	1643.273	57.688	0.146963	73.161	0.186382

Table B: Simulation data for Sample 3 and Sample 4

Load (N)	Stress (MPa)	Sample 3		Sample 4	
		Deflection (mm)	Strain (mm/mm)	Deflection (mm)	Strain (mm/mm)
0	0	0	0	0	0
100	164.3273	1.1221	0.002859	1.1125	0.002834
200	328.6546	2.2441	0.005717	2.2251	0.005669
300	492.9819	3.4856	0.00888	3.4427	0.00877
400	657.3091	5.6152	0.014305	5.4583	0.013905
500	821.6364	9.4726	0.024132	9.005	0.022941
600	985.9637	15.496	0.039477	14.588	0.037164
700	1150.291	24.88	0.063383	23.762	0.060535
800	1314.618	38.58	0.098285	37.264	0.094932
900	1478.946	56.069	0.142839	54.7	0.139351
1000	1643.273	76.631	0.195222	75.36	0.191984

Table C: Simulation data for Sample 5 and Sample 6

Load (N)	Stress (MPa)	Sample 5		Sample 6	
		Deflection (mm)	Strain (mm/mm)	Deflection (mm)	Strain (mm/mm)
0	0	0	0	0	0
100	164.3273	1.3728	0.003497	1.4327	0.00365
200	328.6546	2.7456	0.006995	2.8654	0.0073
300	492.9819	4.3414	0.01106	4.6141	0.011755
400	657.3091	6.9396	0.017679	7.7203	0.019668
500	821.6364	10.845	0.027628	12.513	0.031878
600	985.9637	16.759	0.042694	19.445	0.049537
700	1150.291	26.469	0.067431	30.083	0.076638
800	1314.618	40.408	0.102942	44.371	0.113038
900	1478.946	58.022	0.147814	62.43	0.159044
1000	1643.273	78.798	0.200742	83.568	0.212894

Table D: Simulation data for Sample 7 and Sample 8

Load (N)	Stress (MPa)	Sample 7		Sample 8	
		Deflection (mm)	Strain (mm/mm)	Deflection (mm)	Strain (mm/mm)
0	0	0	0	0	0
100	164.3273	1.4166	0.003609	1.1487	0.002926
200	328.6546	2.8332	0.007218	2.2974	0.005853
300	492.9819	4.5239	0.011525	3.4545	0.008801
400	657.3091	7.4313	0.018932	4.8866	0.012449
500	821.6364	11.881	0.030267	7.1768	0.018283
600	985.9637	18.44	0.046977	11.064	0.028186
700	1150.291	28.685	0.073077	18.475	0.047066
800	1314.618	43.015	0.109583	30.676	0.078149
900	1478.946	60.978	0.155345	47.679	0.121465
1000	1643.273	82.103	0.209162	68.189	0.173715

Table E: Simulation data for Sample 9 and Sample 10

Load (N)	Stress (MPa)	Sample 9		Sample 10	
		Deflection (mm)	Strain (mm/mm)	Deflection (mm)	Strain (mm/mm)
0	0	0	0	0	0
100	164.3273	1.1876	0.003025	1.2922	0.003292
200	328.6546	2.3753	0.006051	2.5844	0.006584
300	492.9819	3.5802	0.009121	4.3058	0.010969
400	657.3091	5.1385	0.013091	7.3736	0.018785
500	821.6364	7.8674	0.020043	12.333	0.031419
600	985.9637	12.405	0.031602	20.18	0.05141
700	1150.291	20.325	0.051779	30.937	0.078814
800	1314.618	32.829	0.083634	44.991	0.114617
900	1478.946	50.035	0.127467	44.991	0.114617
1000	1643.273	70.801	0.180369	83.242	0.212064

Table F: Simulation data for Sample 11 and Sample 12

Load (N)	Stress (MPa)	Sample 11		Sample 12	
		Deflection (mm)	Strain (mm/mm)	Deflection (mm)	Strain (mm/mm)
0	0	0	0	0	0
100	164.3273	1.4214	0.003621	0.88686	0.002259
200	328.6546	2.8429	0.007242	1.7737	0.004519
300	492.9819	4.557	0.011609	2.6613	0.00678
400	657.3091	7.9075	0.020145	3.7408	0.00953
500	821.6364	13.194	0.033612	5.5539	0.014149
600	985.9637	21.503	0.05478	9.1452	0.023298
700	1150.291	32.574	0.082984	15.934	0.040593
800	1314.618	46.894	0.119465	27.827	0.070891
900	1478.946	64.549	0.164442	44.228	0.112673
1000	1643.273	84.992	0.216522	64.225	0.163617